Plasma Physics Reports, Vol. 29, No. 7, 2003, pp. 561–565. From Fizika Plazmy, Vol. 29, No. 7, 2003, pp. 606–611.

NONLINEAR PHENOMENA

On the Efficiency of ELF/VLF Generation Using HF Heating of the Auroral Electrojet[1]

K. Papadopoulos[1, 2], T. Wallace[1], M. McCarrick[1], G. M. Milikh[1, 2], and X. Yang[1]

[1] *Advanced Power Technologies Inc., Washington, DC, USA*

[2] *University of Maryland, College Park, MD, USA*

Received October 24, 2002

Abstract—Using experimental measurements and theoretical analysis, it is shown that the HF/ELF conversion efficiency is controlled by the timescale for electron temperature saturation. This is a function of the ERP and frequency of the heater and the ionospheric electron density profile. For the current HAARP parameters, this corresponds to frequencies between 2 and 4 kHz. Efficiency optimization techniques as applied to the projected upgrading of the HAARP heater to its design power of 3.6 MW are discussed. © *2003 MAIK "Nauka/Interperiodica".*

1. INTRODUCTION

A fundamental plasma physics concept among the main pioneering by Leonid Rudakov was the concept of electron magnetohydrodynamics (EMHD) [1]. The work presented here is a classic example of EMHD application in the Earth's ionosphere, in general, and in the electrojet, in particular.

Electron Hall currents driven by ionospheric electric fields in the D-region of the high latitude zone are responsible for a most fascinating plasma property: the potential to act as a frequency transformer that converts HF power injected from a high power HF transmitter into the ionosphere into coherent lower frequency VLF/ELF/ULF waves. The conversion principle relies on modulating the electrojet currents in the ionospheric D and E regions by using amplitude-modulated HF heating. The low-frequency fields subsequently couple to the earth–ionosphere wave guide, while a fraction of their power leaks towards the magnetosphere. Despite several years of theoretical [2–10] and experimental [11–16] work, many scientific and technical issues remain unresolved. Understanding the physics underlying their generation is important in increasing the HF to ELF/VLF conversion efficiency and utilizing this technique for ionospheric diagnostics. A puzzling feature of the experiments has been the variation of the conversion efficiency with frequency and the unusually large relative amplitude of the harmonics. Figure 1 shows the frequency dependence of the average field amplitude normalized to the amplitude at 2 kHz measured near the HAARP site. These data are typical of many other measurements and consistent with the data reported using the EISCAT heater [12]. The most important features seen in Fig. 1 and from previous data are the following:

(1) An enhanced efficiency relative to the neighboring frequencies at 2 kHz and its harmonics.

(2) If we ignore the enhanced regions, the maximum efficiency is in the frequency range between 2 and 4 kHz. The efficiency is proportional to the frequency f between 2 kHz and 500 Hz. There is a weak increase in the efficiency between 500 and 100 Hz. The efficiency is proportional to $1/f$ between 4 and 10 kHz.

(3) Harmonics with significant relative amplitudes up to ten or larger are present. The amplitudes of the harmonics are much higher than expected from the Fourier analysis of the HF heating waveforms.

Although the various sets of data have been collected under different heating parameters and iono-

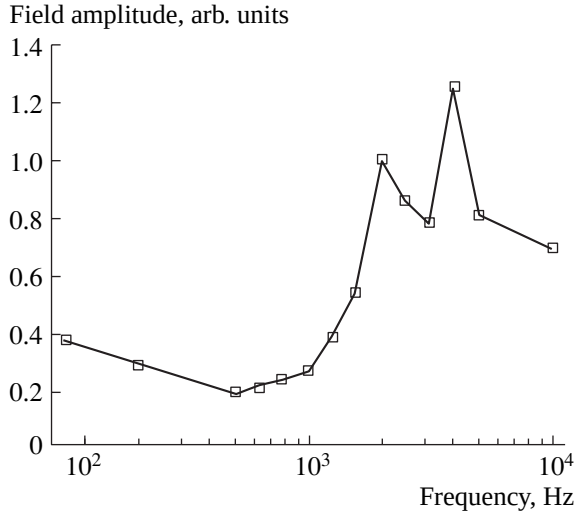

Fig. 1. The average field amplitude measured near the HAARP site versus the ELF/VLF frequency. The amplitude is normalized.

[1] This article was submitted by the authors in English.

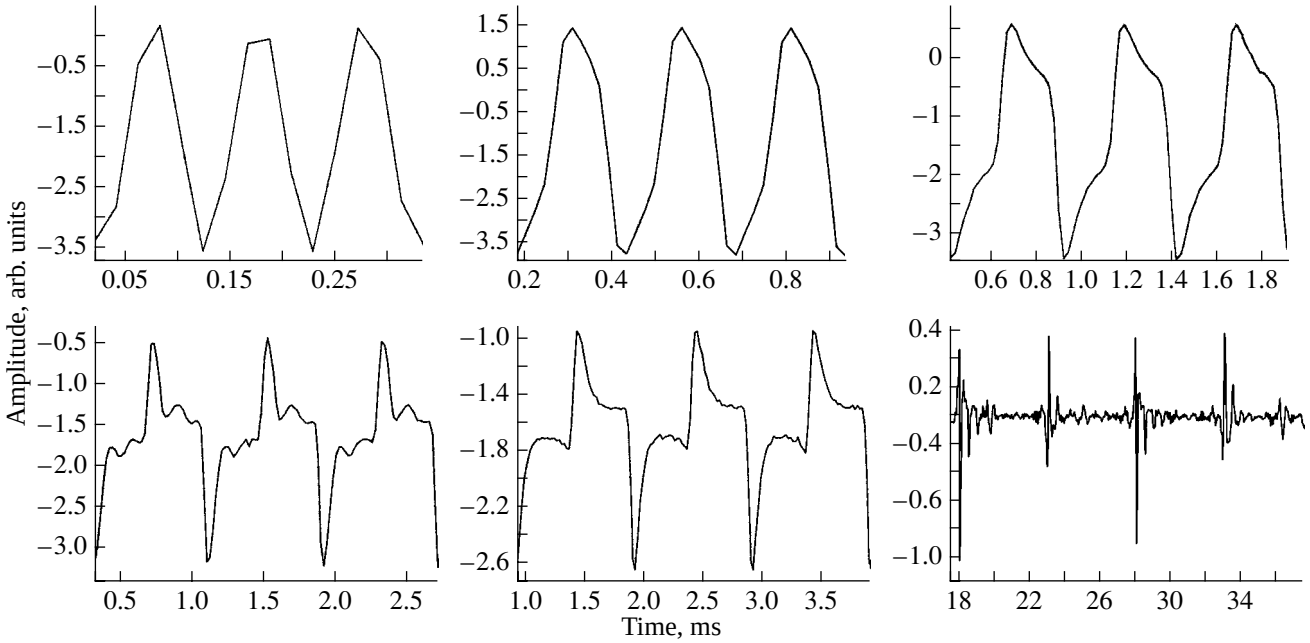

Fig. 2. Temporally resolved waveforms for the N–S components of the magnetic field recorded on March 4, 2001.

spheric conditions, the features described above are very consistent.

As discussed previously [2, 6, 7] and in the absence of propagation effects, the conversion efficiency depends on the value of the ambient electric field in the modified region and the spatiotemporal behavior of the modified conductivity in response to the HF heating pulse. Since the first factor, which basically controls the maximum value of the modified current, is beyond our control, our investigation focused on understanding the physics of the second factor. We present below the first temporally resolved ELF/VLF waveforms measured during modulated ionospheric heating. The results are compared with theoretical models and their implications are discussed.

2. EXPERIMENTAL RESULTS

The data presented below were obtained using the HAARP heater in Gakona, Alaska, during two campaigns. The first involved 48 hours of operation during the period September 17–30, 2000; and the second, 68 hours of operation during the period March 4–14, 2001. In all the results presented here, the heater operated at 3.3 MHz in the X-mode with power 960 kW and ERP 73 dBW. Since we are interested in near-field effects, the ELF/VLF data were recorded at a diagnostic trailer site located 12 km away from the heater. The magnetic fields were measured with EMI BF–6 sensors oriented along the magnetic N–S and E–W directions. The sensor output was digitized at a 24-bit resolution with a 48 kHz sampling frequency, giving temporal resolution of 20 μs in the measured ELF/VLF waveform. They were generated using square-wave HF amplitude modulation between 100 Hz and 10 kHz.

Figure 2 shows temporally resolved waveforms for the dominant magnetic field component (N–S) for the frequencies recorded on March 4 between 05.32 UT and 06:00 UT. Two things are apparent. First, the peak value of amplitude is minimum at 10 kHz. The peak value increases at lower frequencies and reaches a saturation value at a frequency of 4 kHz. Second, the waveforms in the VLF range have significant power in the fundamental frequency. However they deteriorate significantly at the ELF range (1 kHz or lower). Note that in this frequency region the waveform is composed of a spike with duration of 0.125 ms at the beginning of each cycle, followed by a plateau of approximately one-third of the peak amplitude for the remaining pulse. As a result, at low frequencies, the HF-to-ELF conversion is low for most of the cycle. Furthermore, a Fourier analysis of the waveforms is consistent with the presence of harmonics with anomalously high amplitudes.

An additional feature revealed by these data is the presence of weaker peaks with a form similar to the driven waveform with a delay time of approximately 0.5 ms. The last feature was previously reported in [11, 17] and correctly interpreted as echoes generated by the reflection of the original pulse from the ionosphere. Rietveld *et al.* [11] have used these features to determine the ionospheric reflection height and the reflection coefficient and access the heating and cooling times in the D region. The data show the appearance of a plateau in the magnetic field with amplitude approximately 0.3 of the maximum, similar to the plateau

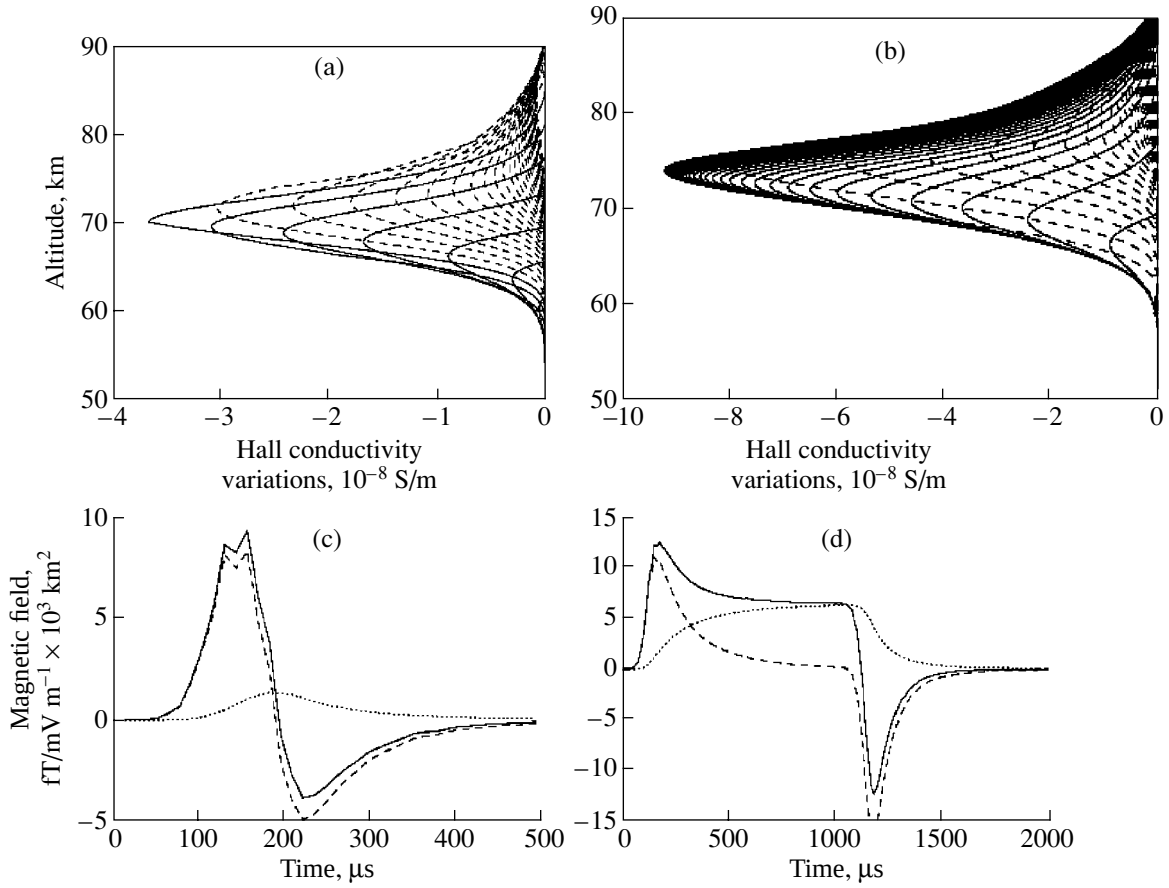

Fig. 3. Variations of the Hall conductivity caused by HF pulses with durations of (a) 50 and (b) 100 μs. Here the solid and broken lines show conductivities produced at the time of HF heating and after the pulse termination, respectively. Plots (c) and (d) reveal the associated temporal evolution of the magnetic field on the ground computed per 1 mV/m of the ambient electric field and per 1000 km^2 of the HF heated area.

shown in Fig. 2 for the ELF range of frequencies. The echoes feature is superimposed on the plateau for pulses longer than 0.5 ms. Referring to Fig. 2 in [17], we note that the plateau region is either lost in the noise or filtered by a low-pass filter. The rest of their waveform is similar to ours.

The ionospheric diagnostics was provided by a digital ionosonde, a magnetometer, and a 30-MHz riometer. During the testing period, the HAARP fluxgate magnetometer showed a moderate 50 gammas predominantly westward magnetic field and a corresponding southward electrojet current. The 30-MHz riometer absorption was about 0.5 dB, corresponding to a nighttime ionospheric profile.

3. THEORETICAL MODELING

The physics underlying these observations can be understood by referring to theoretical modeling. There are two steps in the computation. The first is to find the spatial-temporal profile of the current $\mathbf{j}(\mathbf{r}, t)$ induced by the heater. The second is to compute the near field at the observation site, which we take as the origin of the coordinate system, using a retarded potential method described by the following set of equations:

$$\mathbf{A}(0, t) = \int \frac{\mathbf{j}(r, t - r/c)}{4\pi\varepsilon_0 c^2 r} d\mathbf{r} \tag{1}$$

$$\mathbf{B}(\mathbf{r}, t) = \nabla \times \mathbf{A}(\mathbf{r}, t). \tag{2}$$

From these equations and assuming the ambient electric field E_0 in the x direction, the magnetic fields at the observation point per unit area and per unit electric field are given by

$$B_x(0, t)/SE_0k = \int \left[\frac{\Delta\sigma_H(z, t - z/c)}{z^2} + \frac{\Delta\dot{\sigma}_H(z, t - z/c)}{cz} \right] dz \tag{3}$$

$$B_y(0, t)/SE_0k = \int \left[\frac{\Delta\sigma_P(z, t - z/c)}{z^2} + \frac{\Delta\dot{\sigma}_P(z, t - z/c)}{cz} \right] dz, \tag{4}$$

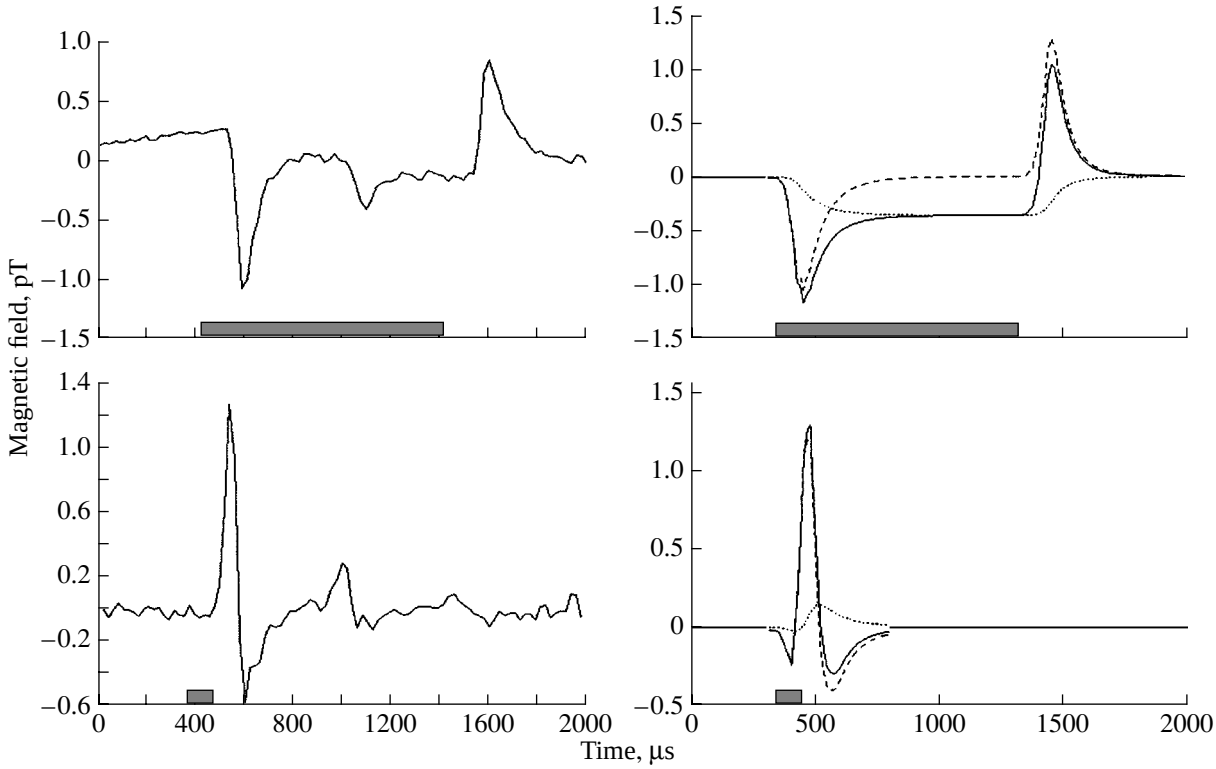

Fig. 4. Experimental results (left column) along with the theoretical predictions (right column) for pulses with durations 1000 μs (on the top) and 50 μs (on the bottom).

where $\sigma_{H,P}$ are the Hall and Pedersen conductivities, S is the HF heated area, $k = 1/4\pi\varepsilon_0 c^2$, ε_0 is permittivity of free space, and $\Delta\dot{\sigma}_{P,H}$ represents derivative with respect to the retarded time. Note that the first term in the square brackets in Eqs. (3) and (4) describes the magnetic field due to the ionospheric current induced by the HF heating, while the second term is due to the time derivative of the current.

The spatial-temporal profile of the conductivity can be found by using 1D HF heating code, such as the one described in APTI, Technical Report 5007, 1991. The inputs to this code are the electron density profile as a function of altitude and the effective radiated power (ERP), frequency, polarization, and modulation format of the heater. A number of ionospheric profiles similar to the ones discussed in [18] are used depending on the value the riometer absorption. In the code, the effects of changing electron temperatures and the ionospheric absorption characteristics are calculated in a self-consistent manner. The output of the code is shown in Fig. 3, for a profile consistent with the experimental times shown in Fig. 2. They were computed for ERP = 73 dBW with a 12.5 μs time step. Figures 3a and 3b reveal the modified Hall conductivity as a function of time for pulse lengths of 0.05 ms and 1.0 ms, while Figs. 3c and 3d display the associated temporal evolution of the magnetic field on the ground. As shown in Figs. 3c and 3d the total field, represented by the continuous line, is composed of two contributions corresponding to the two terms in Eq. (3) and (4). Furthermore, the dotted line indicates the input from the ionospheric current, as discussed above after Eq. (4), while the slashed line exhibits the input from its derivative. It clearly explains the behavior observed in Fig. 3.

For times shorter than 0.125 ms, the second term—the time derivative of the induced ionospheric current—dominates, while at later times this term approaches zero and the dominant contribution is due to the current itself. Furthermore the HF-to-ELF/VLF conversion efficiency is by about 10 dB higher in the first 0.125 ms than the rest of the cycle. This is connected with the saturation of the electron temperature and the conductivity that is dependent only on the intensity of the heating wave at the absorption altitude.

To compare quantitatively the experimental results of Fig. 4 with the theoretical predictions, we took the area $S = 1300$ km^2, consistent with the HAARP antenna gain at 3.3 MHz. Since we could not measure the ambient electric field, we normalized the theoretical value of the magnetic-field peak achieved after 0.125 ms of heating to the experimentally observed value. In understanding Fig. 4, we have to note that the second spike in the experimental data, which appears approximately 1 ms after the main spike, represents the ionospheric reflection of the signal. This effect is not included in the current model.

As Fig. 4 shows, the theoretical and experimental waveforms are in good agreement. Similar agreement was found for the other pulse lengths, as well as for the rest of the experimental times. We should remark that the results of Fig. 4 imply a value of the ambient electric field of about 30 mV/m.

4. CONCLUSIONS

Temporally resolved ELF/VLF waveforms obtained during recent experiments at HAARP show that the efficiency of ELF/VLF generation by the ionospheric HF heating peaks at 2–4 kHz. In order to interpret the experimental results, a new model of ELF/VLF generation by pulsed ionospheric HF heating is presented. This model consists of two elements. The first is the 1D numerical code that computes the electron heating along with the modifications of the conductivity tensor in the ionosphere. The output of this code is fed into a model that computes the magnetic field in the near zone of the virtual ionospheric antenna caused by the HF heating. The magnetic field computed by the model is checked against observations made at the HAARP site. The overall agreement is very good, which implies that our model includes the essential physics and can be used to guide further studies and heater design.

Studies of waveforms show that the saturated heating is the cause of the inefficiency of the ELF production. In order to increase the HF-to-ELF/VLF conversion efficiency, we are planning to apply such techniques as painting, frequency chirping, or fast sweeping.

ACKNOWLEDGMENTS

Over the years, K.P. and G.M. had the privilege and good fortune to have Leonid Rudakov as a friend and colleague. Their long discussions in the US, in Moscow, and at conferences over the world have been instrumental in our scientific work. The above paper owns a lot to their discussions. On his day we wish him the best. The work was supported by the HAARP Program.

REFERENCES

1. A. V. Gordeev, A. S. Kingsep, and L. I. Rudakov, Phys. Rep. **253** (5), 1 (1994).
2. R. Barr and P. Stubbe, Radio Sci. **19**, 1111 (1984).
3. H. G. James, J. Atmos. Terr. Phys. **47**, 1129 (1985).
4. V. K. Tripathi, C. L. Chang, and K. Papadopoulos, Radio Sci. **17**, 1321 (1982).
5. V. M. Sorokin and A. K. Yashenko, Radiophys. Quantum Electron. **35**, 247 (1990).
6. K. Papadopoulos, A. S. Sharma, and C. L. Chang, Comm. Plasma Phys. Control. Fusion **13**, 1 (1989).
7. K. Papadopoulos, C. L. Chang, P. Vitello, and A. Drobot, Radio Sci. **25**, 1311 (1990).
8. G. M. Milikh, K. Papadopoulos, M. McCarrick, and J. Preston, Radiophys. Quantum Electron. **42**, 728 (1999).
9. H. B. Zhou, K. Papadopoulos, A. S. Sharma, and C. L. Chang, Phys. Plasmas **3**, 1484 (1996).
10. H. L. Rowland, J. Geophys. Res. **104**, 4319 (1999).
11. M. T. Rietveld, H. Kopka, and P. Stubbe, J. Atmos. Terr. Phys. **48**, 311 (1986).
12. M. T. Rietveld, P. Stubbe, and H. Kopka, Radio Sci. **24**, 270 (1989).
13. A. J. Ferraro, H. S. Lee, T. W. Collins, *et al.*, IEEE Trans. Antennas Propag. **37**, 802 (1989).
14. M. McCarrick, D. D. Sentman, A. Y. Wong, *et al.*, Radio Sci. **25**, 1291 (1990).
15. R. Barr and P. Stubbe, Geophys. Res. Lett. **18**, 1035 (1991).
16. L. F. Mironenko, V. O. Rapoport, S. N. Mityakov, and D. S. Kotik, Radiophys. Quantum Electron. **41**, 196 (1998).
17. M. T. Rietveld and P. Stubbe, Radio Sci. **22**, 1084 (1987).
18. M. T. Rietveld, H.-P. Mauelshagen, P. Stubbe, *et al.*, J. Geophys. Res. **92**, 8707 (1987).